Amyloid- Peptide–Lipid Bilayer Interaction Investigated by Supercritical Angle Fluorescence

Dubois, Valentin ; Serrano, Diana ; Seeger, Stefan

Abstract: The understanding of the interaction between the membrane of neurons and amyloid-beta peptides is of crucial importance to shed light on the mechanism of toxicity in Alzheimer's disease. This paper describes how supercritical angle fluorescence spectroscopy was applied to monitor in real-time the interaction between a supported lipid bilayer (SLB) and the peptide. Different forms of amyloid-beta (40 and 42 amino acids composition) were tested, and the interfacial fluorescence was measured to get information about the lipid integrity and mobility. The results show a concentration-dependent damaging process of the lipid bilayer. Prolonged interaction with the peptide up to 48 h lead to an extraction and clustering of lipid molecules from the surface and a potential disruption of the bilayer, correlated with the formation of peptide aggregates. The natural diffusion of the lipid was slightly hindered by the interaction with amyloid-beta(1-42) and closely related to the oligomerization of the peptide. The adsorption and desorption of Amyloid-beta was also characterized in terms of affinity. Amyloid-beta(1-42) exhibited a slightly higher affinity than amyloid-beta(1-40). The former was also more prone to aggregate and to adsorb on the bilayer as oligomer.

DOI: https://doi.org/10.1021/acschemneuro.9b00264

Amyloid-β Peptide-Lipid Bilayer Interaction investigated by Supercritical Angle Fluorescence

Valentin Dubois[a], Diana Serrano[a], and Stefan Seeger[a]

[a]Department of Chemistry, University of Zürich, Winterthurerstrasse 190, CH-8057 Zürich, Switzerland

ABSTRACT

The understanding of the interaction between the membrane of neurons and Amyloid-β peptides is of crucial importance to shed light on the mechanism of toxicity in Alzheimer disease. This paper describes how supercritical angle fluorescence spectroscopy was applied to monitor in real-time the interaction between a supported lipid bilayer (SLB) and the peptide. Different forms of Amyloid-β (40 and 42 amino acids composition) were tested and the interfacial fluorescence was measured to get information about the lipid integrity and mobility. The results show a concentration-dependent damaging process of the lipid bilayer. Prolonged interaction with the peptide up to 48 hours lead to an extraction and clustering of lipid molecules from the surface and a potential disruption of the bilayer, correlated with the formation of peptide aggregates. The natural diffusion of the lipid was slightly hindered by the interaction with Amyloid-β(1-42) and closely related to the oligomerization of the peptide. The adsorption and desorption of Amyloid-β was also characterized in terms of affinity. Amyloid-β(1-42) exhibited a slightly higher affinity than Amyloid-β(1-40). The former was also more prone to aggregate and to adsorb on the bilayer as oligomer.

Keywords: amyloid-β, Alzheimer, supported lipid bilayer, fluorescence, interface, supercritical angle fluorescence.

1. INTRODUCTION

Functions of proteins and polypeptide chains are intrinsically based on their three-dimensional structure. Whatever the structure is, it is reached in vivo in a short time scale after the synthesis of the molecule, driven by stabilizing non-covalent interactions between the amino acids[1,2]. This process is referred to as protein folding. However, incorrect conformations might be the result of improper folding and be stable enough to hinder any restructuration toward the correct functional structure[3]. These "misfolded" polypeptides are likely to promote health troubles either by canceling necessary biological functions or gaining toxic properties[4]. Misfolded or disordered polypeptides sometimes aggregate into a specific structure called "amyloid fibril". This amyloid fibril is characterized by a stack of β-sheet strands forming a cross-β structure perpendicular to the axis of fibril growth[5,6]. Several diseases are correlated to the formation and deposition of such amyloid structure, either intra or extracellular[5,7,8]. Among them, Alzheimer is a neurodegenerative disease of particular interest and is recognized by extracellular deposition of aggregated amyloid-β peptides (Aβ) as plaque composed of amyloid fibrils surrounding the neurons[9].

Aβ is a small peptide generated by the cleavage of a transmembrane protein called amyloid-β precursor protein (APP). The resulting Aβ fragments vary in their length but the most commonly found in Alzheimer plaque count 40 or 42 amino acids[10,11]. The native structure of Aβ is usually described either as a random coil in aqueous solution[12] or as a small α-helix when interacting with membrane or hydrophobic surfaces[13,14]. According to recent theories, the small oligomers formed in the early stage of aggregation are supposed to be more toxic for the neurons than the late fibrillar aggregates which constitute the extracellular plaque[15–17]. However, the direct cause for toxicity remains unclear. Different effects have been observed following the aggregation of the peptides and could explain the neuronal death encountered in the brain of disease patients. These effects include the oxidation of the lipid molecules in the membrane[18,19], hindrance of the lipids mobility within the bilayer[20] and formation of pore-like channels through the membrane of cells[15,21,22].

Different *in vitro* lipid structures have been established to study the impact of their interaction with peptides, assuming that these models can partially mimic the response of neuron membrane *in vivo*[23,24]. Among these models, supported lipid bilayers (SLB) are planar fluid membranes formed by deposition and fusion of unilamellar vesicles (ULVs) onto hydrophilic substrates[25]. SLBs are easily formed on a support and are attractive due to their simplicity compared to cell membranes. Furthermore, their formation takes place directly on an interface between the support and the sample medium. This last feature makes the SLB model particularly suitable for surface sensitive techniques since the interaction with peptides will occur only within this interfacial region. Supercritical angle fluorescence (SAF) is one of these selective techniques. It allows to distinguish between fluorophores emitting a signal from the interface and those which are diffusing in the bulk solution, without the need of any washing steps to remove unbound molecules. Therefore, real-time monitoring of interaction processes is possible including recording kinetic data. This is achieved by specifically collecting the fluorescence coming from above the angle of total internal reflection (critical angle) of a glass-water interface, essentially emitted by the fluorophores situated near such an interface. Therefore, it excludes almost all fluorescence which is emitted beyond a range of ~200 nm from the surface[26,27]. In addition, undercritical angle fluorescence (UAF) can be collected simultaneously. This signal corresponds to the output of a traditional confocal microscope. It allows to detect fluorophores emitting from the bulk solution with a collection efficiency extending up to ~2.5 µm above the interface[28].
The simultaneous detection of SAF and UAF signal even allows the precise determination of the position of an emitter in the axial direction from the surface, i.e. a precision down to a few nanometers. This technique has been already applied to study the interaction of α-synuclein[29]. SAF has also been developed for special fluorescence methods, e.g. SAF-FRET and SAF-FCS[30]. The SAF/UAF technique was used in this study to investigate the interaction between a negatively charged SLB and two different Aβ 40 and 42 amino acids long peptides, referred to as Aβ(1-40) and Aβ(1-42) respectively. Among these peptides, Aβ(1-42) was assumed to be potentially more toxic since it would have a higher propensity to aggregate into oligomers[31].

2. RESULTS AND DISCUSSION

2.1 Adsorption affinity of the peptides.

In a first experiment we studied in real-time the affinity of Aβ to SLBs by SAF. In order to quantify the early-stage adsorption, non-fluorescent SLBs were incubated with fluorescently labelled peptide solutions (Aβ (1-40) and Aβ (1-42)). Similar fluorescent labels were proven by Quinn et al. to yield analogous structures for aggregated Aβ and the unlabelled peptides[32,33]. Furthermore, in each sample only 1% of the peptides added were fluorescently labelled. Such amount limited the influence of the label moieties on the aggregation of other peptides. It also prevented fluorescence self-quenching and provided satisfying signal. Because the SAF channel only transmits photons arising from the interface, the signal was considered as the emission of SLB-bound peptides only. The SAF signal was monitored over a certain area for different peptide concentrations ranging from 1 µM to 40 µM during at least 6 hours after the beginning of the incubation. The intensity of fluorescence was averaged over the complete area of each scan. The change in fluorescence intensity recorded from the SAF channel was plotted as a function of the incubation time (Fig. 1 a). Results revealed a particular evolution of the signal divided in two time-ranges. For an incubation time up to 30 minutes, all protein solutions showed a fast increase in fluorescence intensity, followed by a systematic decrease in intensity. These results are interpreted as a fast adsorption of the peptides followed by a partial desorption due to weak unspecific interactions. This behavior is well known as “overshooting” and known also from the adsorption of other proteins[34–37]. This time range is hereafter referred to as short-time adsorption (depicted by the red shade on Fig. 1 a). During the short-time adsorption, Aβ (1-40) displayed a higher fluorescence signal than its more toxic counterpart Aβ (1-42) for concentrations between 1 µM and 5 µM (Fig. 1 b). However, this tendency was reversed beyond 10 µM, namely at concentration equal or superior to the critical micellar concentration (cmc) of both Aβ’s[38]. Around and beyond cmc range Aβ (1-42) is known to exist as higher order aggregates than Aβ (1-40). This explains its subsequent higher fluorescence intensity during overshooting since the first adsorbed peptides are bigger aggregates (cfr. supporting information, S1). Once the minima of SAF intensity have been reached after the overshooting effect described previously, extended time of adsorption yielded in different behavior for each type of peptide. Aβ (1-40) exhibited either a plateau or a slow increase when the time of incubation was prolonged beyond 24h.

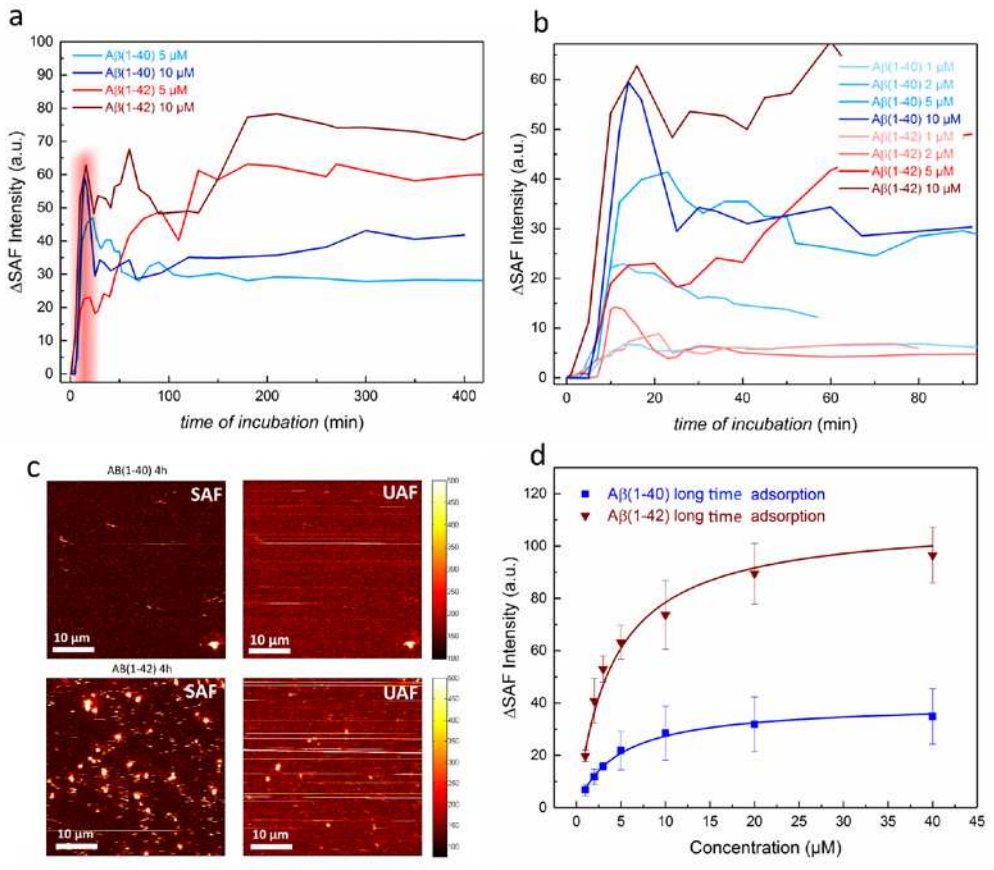

Figure 1. Evolution of the SAF signal after incubation with fluorescent peptides. (a) Long-time adsorption of Aβ (1-40) and Aβ (1-42). Short-time adsorption is highlighted in red. (b) Short-time adsorption/overshooting period of Aβ (1-40) and Aβ (1-42). (c) Comparison between SAF/UAF imaging of 5 µM Aβ (1-40) and Aβ (1-42) after 4 hours of incubation. (d) Maxima of fluorescence intensity after 6 hours of incubation as a function of Aβ concentration.

On the other hand, Aβ (1-42) showed a further increase in fluorescence intensity after only one hour. Aβ (1-42) exhibits several irregular jumps of intensity before reaching another plateau. SAF imaging of the surface area allowed to correlate these fluctuations with the appearance of fluorescent aggregates on the SLB (Fig. 1 c). On the UAF imaging, bright stripes are visible which are attributed to the motion of these fluorescent aggregates in the bulk solution during the scanning process. Some of them will eventually adsorb durably on the interface and increase the SAF intensity. Also, some of the aggregates were less intense or seemingly absent from the UAF channel. This situation corresponds to fluorophores detected closer from the interface, whose fluorescence radiations are mostly sent above the critical angle[27]. The part of their emission which is detected under the critical angle (UAF) is therefore smaller and they are harder to distinguish from the bulk fluorescence background. These fluorescent aggregates are thought to be the result of peptides oligomerization. As shown by the comparison of imaging between the two peptides, Aβ(1-42) exhibited a stronger and faster tendency than Aβ (1-40) to form these aggregates and nucleation sites of aggregation on top of the SLB after the short-time adsorption/desorption phase. This was especially obvious at concentrations above 5 µM. This outcome is in accordance with previous reports showing the higher propensity of Aβ (1-42) to aggregate, due to the influence of the longer C-terminus [31]. Therefore, the outstanding signal of Aβ(1-42) on the interface after long-time adsorption could have three explanations. It was either due to the adsorption on the SLB of peptide aggregates pre-formed in solution ; or caused by peptides stacking on aggregates already adsorbed ; and/or simply caused by an enhanced adsorption of monomers due to a higher affinity for the lipids. The quantification of Aβ(1-40) and Aβ(1-42) affinities was required to assess this hypothesis. To quantify the affinity of the peptides for the SLB, the maximum of average intensity of the area after 6h of adsorption was plotted as a function of peptide concentration (Fig. 1 d). This curve was then fitted with a Langmuir isotherm[39]

(Equation 1). Fitting yielded values for the unspecific adsorption constant (K_u), which were then expressed as dissociation constant (K_d) to quantify this affinity (Equation 2).

$$I = I_{max} \frac{K_u \cdot C}{K_u \cdot C + 1} \quad (1)$$

$$K_u = \frac{k_a}{k_d} = \frac{1}{K_d} \quad (2)$$

where I is the measured fluorescence intensity, I_{max} is the maximum fluorescence intensity reached at higher concentration, and k_a, k_b being the kinetic constants for unspecific adsorption and desorption respectively. The values calculated for K_d were $(4.24 \pm 0.28) \times 10^{-6}$ M for Aβ(1-40) and $(3.48 \pm 0.37) \times 10^{-6}$ M for Aβ(1-42). Despite the high limitation of the Langmuir isotherm model to describe protein adsorption events, the range of these values is in accordance with other studies[40,41]. From these data, it is supposed that the slightly higher K_d value for Aβ (1-40) reflects a weaker interaction with lipid molecules than Aβ(1-42). This could be expected for the less toxic type of peptide, although the difference of affinity is too small to justify the discrepancies in SAF. Despite having similar values for K_d, the I_{max} of each peptide is drastically different, as shown in Fig. 1 c: the maximum SAF intensity of Aβ(1-42) is almost 3-folds higher than its counterpart. During these experiments, Aβ(1-42) reached a higher SAF intensity than Aβ(1-40) when aggregates became visible on the interface. From that moment, the SAF intensity increased until a plateau is reached, demonstrating that the aggregates are adsorbed durably and not reversibly. Since our results yielded a similar affinity of both peptides for the lipids, this increase of surface fluorescence is likely the consequence of the deposition and subsequent growth of these aggregates. More Aβ(1-42) adsorbed on the surface than Aβ(1-40) because they were in oligomeric state. So, the higher affinity of Aβ(1-42) for the SLB is nothing but a secondary factor to explain its higher SAF signal. The fact that Aβ (1-42) is the prior component of senile plaques in the brain[42,43] supports the hypothesis that it aggregates more rapidly than Aβ(1-40) and interacts durably with the lipids at the early stage of the disease, while Aβ(1-40) is slower to oligomerize. In the absence of oligomers, the maximum adsorption of non-aggregated peptides is limited by the saturation of the surface with monomers. The adsorption of monomers is also reversible at least at the initial (overshooting) period (i.e. desorption is observed up to 30 minutes of incubation). This limitation would explain why a non-aggregating Aβ(1-40) peptide yielded less signal than Aβ(1-42), prone to form oligomers. To confirm this supposition, the evolution and average intensity of the non-aggregated Aβ(1-42) layer was selectively monitored and compared with the data obtained from its aggregates (Fig. 2 a).

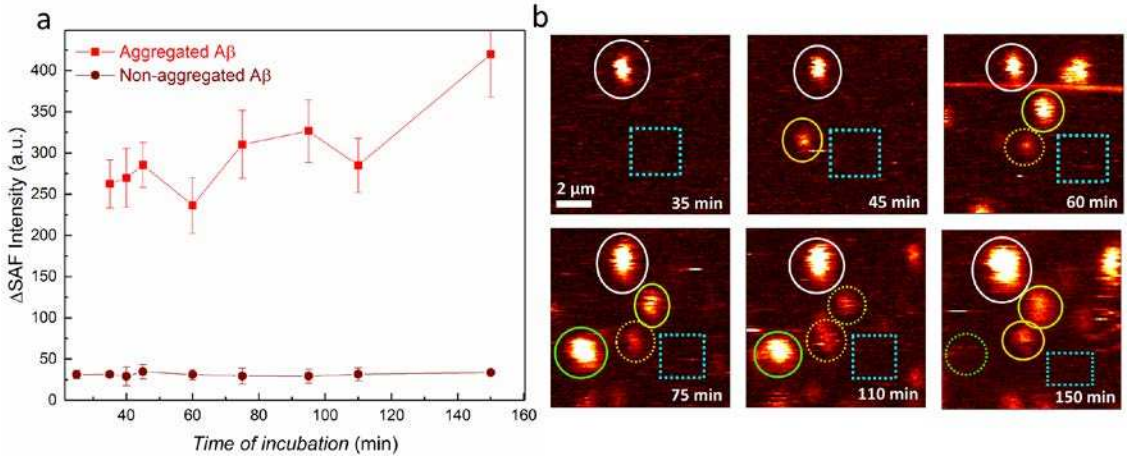

Figure 2. (a) Evolution of SAF intensity as a function of time for non-aggregated layer and aggregated sample of 10 µM fluorescent Aβ(1-42). (b) SAF imaging data with the tracking of the aggregates over time displayed by colored circles (each colored circle correspond to one of the aggregates which remain at similar location). The SAF intensity of the first aggregate (white circle) and non-aggregated area (blue box) are displayed in (a).

From its constant SAF value, it is clear that the layer of adsorbed non-aggregated Aβ is in equilibrium and saturation, respectively, with the incoming flow of peptides once the surface is saturated. Moreover, the SAF intensity of the non-aggregated layer of Aβ(1-42) (Fig. 2 a, bottom line) is similar to the average SAF intensity of Aβ(1-40) in Fig. 1 a,c. This confirms that the presence of Aβ(1-42) aggregate is the main source for the discrepancies in maximum SAF intensity: without these aggregates, the two peptides would exhibit comparable SAF signal. Unlike the non-aggregated peptide areas, the fluorescent aggregates displayed in Fig. 2 b exhibited an increasing intensity. The aggregates are adsorbed tightly enough at the lipid bilayer so that most of them can be "tracked" by SAF imaging. This is represented in Fig. 2 b where each circle corresponds to the follow-up of one aggregate, a dashed circle indicating the same aggregate desorbs. They seemed to spread or desorb punctually, but the lateral position of many of them remained similar over a time-span of more than 2 hours. These measurements confirm the assumption that non-aggregated monomeric Aβ(1-40) and Aβ(1-42) have a similar adsorption affinity. The different adsorption behavior of Aβ(1-40) and Aβ(1-42) arises from the aggregates and not from the monomeric peptides. On the other hand, new interrogations came from the SAF imaging and tracking of the aggregates, whose motion seemed extremely limited. This might have been caused by an immobilization of the peptides on the glass surface, through the SLB. To check the latter hypothesis, the incubation of 10 µM Aβ(1-42) on SLB or on a bare glass slide was compared (cfr. supporting information, S2, S3). The more static aggregates were observed on both surfaces. But on average, the fluctuation of the fluorescent clusters indicated that only few peptides were totally immobilized on glass or on SLB. Comparison between bare glass and SLB also showed a net preferential adsorption of peptides on lipids. Therefore, it seems reasonable to assume that alterations of the membrane are caused by these interactions rather than by artefacts from peptides adsorbed on the glass slide.

2.2 Impact of Aβ adsorption on fluorescently labelled SLBs.

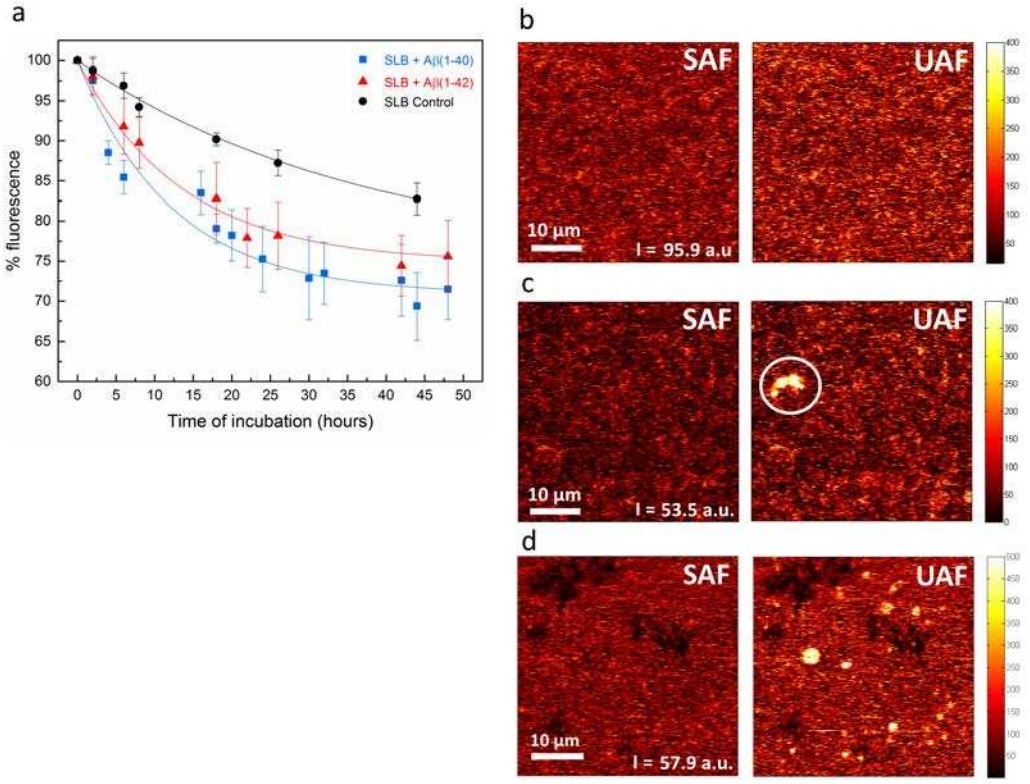

Figure 3. (a) Evolution of the SLB average fluorescence intensity over the time of incubation with 0.5 µM Aβ solutions. (right side) Comparison between SAF and UAF imaging of SLB after 24 h of incubation (b) without peptides (PBS only), (c) with 5 µM Aβ(1-40), (d) with 50 µM Aβ(1-40). The average SAF intensity of the SLB is displayed at the bottom right corner.

To elaborate the impact of the Aβ adsorption on the SLB, the signal from a fluorescently-labelled SLB was monitored upon incubation with unlabeled peptides. Typically, images of the bilayer were recorded periodically in both SAF and UAF channels at different concentrations and at incubation times up to 48 hours. Three different effects could be observed, depending on the concentration of peptides: a decrease of the average SLB fluorescence intensity; the formation of fluorescent lipid aggregates; and eventually the disruption of the bilayer. At concentration between 0.5 and 5 µM, both Aβ (1-40) and Aβ (1-42) promote a decrease in SLB fluorescence intensity over time (Fig. 3 a). A lipid control confirmed that this effect was not only due to photobleaching or natural damaging but indeed reflected an influence of the peptides.

When incubated with Aβ solutions of concentrations beyond 5 µM, the imaging displayed some fluorescent aggregates, attributed to the clustering of lipids (Fig. 3 c). The signal of these lipid clusters was more intense in the UAF than in the SAF channel. This interesting feature can be explained by a protrusion of the lipids growing beyond the interface and the maximum detection efficiency of SAF. Since the protocol for the formation of SLB (section 4.2) includes a washing of most of the unbound lipid vesicles, lipids clusters cannot be due to residual vesicles and are more likely formed from the interfacial lipids themselves which protrude above the bilayer. It is interesting to point out that the minimum Aβ concentration for the formation of these lipid clusters coincide with the minimum concentration at which peptide aggregates were observed (cfr. section 2.1). Therefore, this is an indication that peptide aggregation and lipid clustering are two concerted events. Besides the clustering of lipids, the formation of small dark areas in the SLB could be observed after approximately 20 hours of incubation with 50 µM of peptides. Such dark areas are attributed to a local desorption of the two lipid leaflets from the interface. These "holes" within the SLB had a diameter around 2-3 µm. The formation of smaller pores with a diameter size of 16 nm have been reported after 20 min for Aβ directly mixed with liposomes[44], which is beyond the lateral resolution of the microscope used in this study (550 ± 50 nm). Longer monitoring showed the holes spreading among the SLB and consequently resulted in a bilayer disruption. Beyond 24 hours of monitoring, a real disruption of the bilayer could be observed (Fig. 3 d). From these results it appears that a part of the toxicity of the two amyloidogenic peptides could arise from a progressive and concentration-dependent lipid removal process. The interactions with the peptides can induce an extraction of some lipid molecules from the bilayer, resulting in a decrease of fluorescence and thinning of the membrane when the lipid-peptide complex desorbs from the surface. These extracted lipid molecules can cluster due to the aggregation process between peptides encountered at higher concentration, assuming that each peptide maintains its interaction with extracted lipids while aggregating. At some point, the aggregated lipid-peptide structures may become too massive and unstable to withstand the flow of solution inside the measuring cell, hence being washed away and forming holes within the bilayer. These holes can eventually yield the disruption of the SLB (Fig. 4). This hypothesis is in agreement with other theories despite the discrepancies in SLB compositions, affinities or steady-state experiments within these studies[20,29].

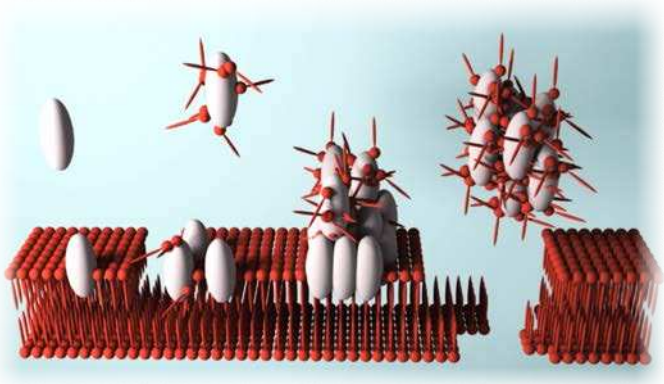

Figure 4. Scheme of the hypothesized mechanism of toxicity of Aβ upon interaction with a lipid bilayer. A progressive and concentration/aggregation-dependent lipid removal process leads to a thinning and potential disruption of the SLB

In addition, these results were observed with two different SLB compositions, one including cholesterol. The only difference observed was the strength of the lipid-desorbing effect (cfr. supporting information, S4). Although a concentration of 50 µM Aβ is physiologically irrelevant[45], lower concentration of the peptide also yielded a loss of fluorescence, which is still attributed to an extraction of lipid molecules. This effect could be sufficient to destabilize the structure of the membrane bilayer by reducing its thickness. Such event can hinder biological functions localized around the membrane and eventually promote cellular death.

2.3 Evolution of the diffusion coefficient of lipids in SLB.

Another important feature of lipid bilayers is the intrinsic mobility of lipid molecules and their lateral diffusion within the lipid leaflets[46,47]. Fluorescently labelled SLBs were studied by supercritical angle fluorescence correlation spectroscopy (SAF-FCS) upon incubation with peptides, using the signal detected by the SAF channel (cfr. supporting information, S5). Correlation plots were then fitted with a 2-dimensional diffusion model. Fitting allowed calculation of the diffusion coefficient (D_L) which quantifies the lateral diffusion of lipid molecules (Equations 3, 4). Control values for SLB composition used in this study were in accordance with analogous data, considering discrepancies between the samples (~3-4×10^{-12}m²s^{-1} for pure DOPC[48] and ~2-3×10^{-12}m²s^{-1} for DMPC[49]). FCS data of SLBs were recorded using different concentrations of Aβ peptide (Table 1). Most of Aβ samples had small impact on the mobility of lipid molecules during our experiments. Even at concentration as high as 50 µM, Aβ(1-40) did not influence the lateral diffusion of the lipids apart from the vicinity of the bilayer disruption. A possible explanation is provided by Ding et al. and their results of fluorescence recovery after photobleaching (FRAP) experiments, showing that the two D_L values, of lipids and Aβ peptides respectively, were close[50]. Similarity between the speed of diffusion of the lipids and Aβ would explain why the peptide has minor influence on the lateral diffusion of the SLB in our experiments. However, the more toxic Aβ(1-42) induced a significant drop of the D_L of our SLB at a concentration of 25 µM. In addition, Aβ(1-42) started to influence the diffusion of lipids after a minimum of 2 hours of incubation and it was known from previous results that after such a delay, Aβ(1-42) would likely have formed aggregates on the surface of the SLB (cfr. section 2.1). It is supposed that the more massive aggregated species were able to slow down the diffusion of the lipids while smaller peptide species previously adsorbed had no influence. The fact that only Aβ(1-42), with a higher propensity to aggregate, exhibited a general impact on the diffusion of lipids support the oligomeric hypothesis. This can be regarded as another proof of the oligomeric nature of toxic Aβ, since the condition for the hindrance of the lipids diffusion coincides with the formation and adsorption of aggregated peptide species.

Table 1. Values of the diffusion coefficient of SLB after 20 hours of incubation with Aβ peptide.

D_L (10^{-12}m²s^{-1})	0.5 µM Aβ(1-40)	5 µM Aβ(1-40)	50 µM Aβ(1-40)	0.5 µM Aβ(1-42)	5 µM Aβ(1-42)	25 µM Aβ(1-42)
Before incubation	2.88 ± 0.22	2.78 ± 0.27	2.91 ± 0.11	2.94 ± 0.42	2.69 ± 0.15	2.95 ± 0.38
After 20 h incubation	3.01 ± 0.10	3.06 ± 0.07	3.14 ± 0.05	2.91 ± 0.40	2.43 ± 0.06	1.90 ± 0.18

2.4 Evolution of the diffusion coefficient of Aβ peptides.

In addition to the mobility of the lipids, the diffusion of Aβ adsorbed at the SLB surface was also measured with fluorescent peptides. The data resulting from the SAF-FCS experiments were fitted to extract the diffusion coefficient. However, the diffusion of Aβ is not limited to the surface. In addition to a lateral diffusion on the surface of SLB, the motion of peptides also includes their adsorption and desorption from the surface. Therefore a 2-dimensional diffusion model was insufficient to evaluate their diffusion properly. Instead, a SAF-3-dimensional model was used. It was elaborated to include the exponential decay of detection of the supercritical angle technique along the axial axis[30] as the peptides diffuse away from the interface. At a concentration of 5 µM the average diffusion coefficient of Aβ(1-40) was (24.85 ± 5.59) × 10^{-12} m^{2}s^{-1} while Aβ(1-42) had an average diffusion coefficient of (2.79 ± 0.49) × 10^{-12} m^{2}s^{-1}. It appears that the diffusion coefficient of Aβ(1-42) is in the range of the D_L calculated for the SLB (table 1) while Aβ(1-40) diffused faster by one order of magnitude. Aβ(1-42) was previously identified as the peptide with a higher affinity for SLB and was adsorbed more tightly, therefore it could be appropriate that this peptide and the lipids diffuse with a similar speed. On the other hand, Aβ(1-40)

is less tightly adsorbed and the amount of peptides within the detection volume fluctuates more rapidly due to faster adsorption/desorption processes. Quantitative comparison between the D_L of the lipids and D_L of Aβ should be made carefully since a 2-dimensional model was used to fit the diffusion of SLB, in contrast with the 3-dimensional SAF model used to fit the diffusion of Aβ. A simple qualitative analysis between the two types of peptide is more relevant, yet it shows explicitly that the SAF intensity of Aβ(1-42) fluctuates less than its shorter counterpart, hence the lower D_L for Aβ(1-42). The major contribution to the fluctuations of intensity is attributed to the adsorption/desorption process inside and outside of the detection volume, rather than a lateral diffusion at the surface of the bilayer. Discrepancies of this adsorption/desorption process between the two peptides can be explained by the difference of affinity for the SLB and the stability of peptide aggregates described in section 2.1. The FCS data obtained show a relation between the number of fluorescent emitters and the diffusion rate. Namely, Aβ(1-42) FCS data suggested a higher number of fluorophores than the signal observed from Aβ(1-40) in the monitored areas (cfr. supporting information, S6). Therefore, the slower diffusion of Aβ(1-42) correlates with a higher density of peptides on the surface, hence higher-order oligomers.

2.5 Influence of calcium ions on the interaction between Aβ and SLB.

The probable bidirectional relationship between Aβ and Ca^{2+} in Alzheimer disease has long been hypothesized[51]. Aβ can disturb Ca^{2+} homeostasis[52], notably by formation of cation-selective channels, as mentioned earlier[53,54]. On the other hand, dysregulation in the dynamics of Ca^{2+} ions can modify the brain metabolism and trigger the release of Aβ peptide[55]. Interactions between Aβ and Ca^{2+} also promotes the formation of oligomeric species[56] and facilitates the binding of the peptide on the membrane[57] via formation of ionic bridges. For all these reasons, the experiments described in previous sections have been repeated using PBS with 2 mM of $CaCl_2 \cdot 3H_2O$. The obtained results have been compared with those including Aβ dissolved in PBS.

First, the monitoring of the adsorption of Aβ dissolved in membrane buffer was reproduced at low concentrations on a SLB. The average fluorescence of the monitored area was measured after 24 hours of incubation with the peptides. As a matter of fact, dissolution in membrane buffer increased the number of adsorbed peptides on SLB, compared with peptides dissolved in PBS (Fig. 5 a). This effect is thought to be the consequence of the interactions between Aβ and calcium ions. Computational studies explain this effect by the formation of the previously mentioned ionic bridge. Ca^{2+} is supposed to act as a link between the polar head group of the lipids and the peptides, negatively charged at neutral pH[58]. It also strengthens the electrostatic interactions between charged residues of Aβ and the SLB[59]. Ca^{2+} also enhanced the amount of aggregated species on the surface, even at concentrations as low as 200 nM (data not showed). This enhancement of peptide aggregation can be expected since the ion-bridge can also occur between two negatively charged peptides. However, the increase of fluorescent adsorbates due to calcium is only partially maintained beyond 2 µM peptides. Aβ(1-40) exhibited the highest enhancement of adsorption at concentrations of 1 and 2 µM, while Aβ(1-42) adsorption was only slightly strengthened at 5 µM. It is expected that beyond 2 µM, the concentration of peptides is sufficient for aggregation to occur in PBS solution without the influence of ion-bridge between Aβ. Therefore, the influence of aggregation on fluorescence intensity is not specific of Ca^{2+} buffer anymore. It is thought that the presence of Ca^{2+} can trigger the aggregation of Aβ and act as a bridge between the peptides and the lipid bilayer. However, the influence of this bridging effect on the adsorption is preponderant only at concentrations lower than 2 µM. Beyond this limit, the flux of peptides coming from the bulk solution toward the membrane is supposed to overcome the influence of the calcium.

Furthermore, Ca^{2+} enhanced the decrease in the fluorescence of SLB observed when interacting with the peptides at 0.5 µM (Fig. 5 b). This outcome has several possible explanations. As Ca^{2+} triggers the oligomerization of Aβ peptide at low concentration, it may promote more damaging within the SLB. Additionally, dynamic simulations showed that calcium ions stimulate a deeper insertion of Aβ inside the bilayer[59], which correlates with a stronger disordering or thinning effect[60,61]. Another explanation is based on the previous conclusion that lipid removal is a concentration-dependent process. Since calcium ions increase the amount of adsorbed peptide – aggregated or not - the amount of extracted lipid molecules would be increased as well. Nevertheless, a conclusion similar to the previous adsorption experiment was drawn when the concentration of peptide was increased to 5 µM. At this concentration, the adsorption and aggregation features of Aβ were almost identical when dissolved in PBS or Ca^{2+} buffer, therefore the impact of the peptide on the SLB did not differ either, no matter in which buffer the peptide was dissolved. Finally, the influence of the peptide on the mobility of the lipid was measured by FCS. The values of D_L of the lipids after incubation with the peptide in the Ca^{2+} containing liquid phase are

close to those obtained when Aβ is dissolved in PBS (Table 2). It was concluded in section 2.3 that the aggregation state of the peptides interacting with the SLB was the critical parameter to influence the diffusion of the lipids. The propensity to aggregate of such highly concentrated peptides interacting with the SLB seemed unaltered by the presence of Ca^{2+} ions, therefore no further reduction of the diffusion coefficient of SLB should be expected, as showed by the experiment.

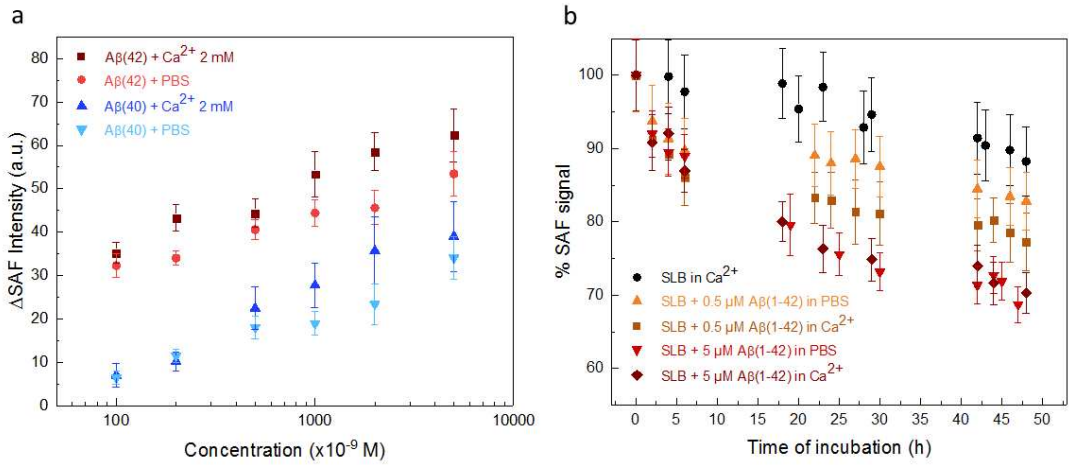

Figure 5. (a) Comparison of the adsorption of labelled peptide incubated over SLB in PBS and with Ca^{2+}. (b) Comparison of the decrease in fluorescence intensity when labelled SLB are incubated with Aβ in PBS and with Ca^{2+}.

Table 2. Comparison of the diffusion coefficient of lipids inside SLB incubated with Aβ(1-42) in PBS and Ca^{2+} .

D_L ($10^{-12}m^2s^{-1}$)	5 μM Aβ(1-42) (in PBS)	25 μM Aβ(1-42) (in PBS)	5 μM Aβ(1-42) (+ 2 mM Ca^{2+})	25 μM Aβ(1-42) (+ 2mM Ca^{2+})
Before incubation	2.69 ± 0.15	2.95 ± 0.38	2.78 ± 0.20	2.81 ± 0.32
After 20 h incubation	2.43 ± 0.06	1.90 ± 0.18	2.39 ± 0.17	2.04 ± 0.22

2.6 Conclusion.

In the present study the interaction between a lipid bilayer and two variants of Aβ peptides, responsible for Alzheimer disease, and also the effect of this interaction on the lipid molecules were investigated. Supercritical angle fluorescence microscopy was used in order to limit the detection volume to an area close to the bilayer interface. First, the adsorption of the peptides on SLB was monitored. From these results, the affinity of each could be calculated. Due to the absence of specific receptors in the bilayer, the interactions were considered as unspecific. As a matter of fact, the calculated values for K_d were in the range of low affinity interactions. Aβ(1-42) seemed to have a slightly higher affinity than the less toxic Aβ(1-40) after an incubation of a few hours, but mostly exhibited a higher tendency to form aggregates upon the bilayer. Further, the impact of such interactions on fluorescently labelled SLBs have been evaluated. Different effects were observed, depending on the concentration: a decrease of fluorescence intensity, a clustering of lipid molecules and eventually the progressive disruption of the bilayer. These effects were independent of which type of Aβ was incubated with the SLB. Despite the fact that these results were obtained with high concentration of peptides, they give an insight in the process which locally reduces the thickness of the bilayer and can make the cell membrane more fragile or even porous (Figure 4). The last step consisted to elaborate the effect of the peptides on the lateral lipid diffusion within the bilayer. Aβ(1-40) seemed to have no effect at all, while high concentration of Aβ(1-42) lead to a decrease in the mobility of lipids. Since the time of incubation, the concentration and the type of peptide required to affect D_L of lipids all coincided with the conditions for maximum aggregation of Aβ, it seems that the hindrance of the diffusion of lipids is correlated with the adsorption of massive oligomeric species. Saturation of the surface with monomers or small oligomers (Fig. 2 b) seemed

unable to affect the diffusion of the lipids. The diffusion of the peptides themselves is also a critical parameter, since only the slowest diffusing peptide Aβ(1-42) affected the diffusion within the SLB.

In order to study the impact of calcium ions on these effects, experiments were repeated with Aβ(1-42) dissolved in a buffer containing 5 mM of Ca^{2+} instead of PBS. The results confirmed previous computational studies which reported an enhanced adsorption of the peptide on the lipids, probably due to the formation of ionic bridges, stronger electrostatic interactions and oligomerization. Calcium ions also increased the loss of fluorescence of labelled SLB incubated with Aβ. It was concluded that Ca^{2+} activates the toxicity of the peptide at low concentration, either by inducing oligomerization or through a deeper insertion within the bilayer. It would be interesting to investigate the latter effect by the use of neutron reflectometry. However, Ca^{2+} buffer did not yield any difference compared to PBS once the Aβ concentration was equal or superior to 5 µM and did not affect the influence of the peptide over the diffusion of the lipids at all. This result suggests that the aggregation process of the peptides was unchanged by Ca^{2+} beyond 5 µM. Therefore, the influence of Ca^{2+} in our experiments was limited at low concentration of peptides for which calcium actually increased the amount of adsorbed peptides, their aggregation and the potential disordering of the SLB. The influence of Ca^{2+} was lost once the concentration of peptide was high enough to yield aggregation in PBS. Higher damaging of SLB, correlated with aggregation at low concentration is another proof of the role of oligomers in the toxicity of Aβ. Eventually, the first stages of Alzheimer disease could correlate with the interactions of low concentrated Aβ with Ca^{2+} near the membrane of neurons. Since the toxic effects of the peptide disturb calcium homeostasis and the ions themselves trigger peptide release and adsorption, it could be a progressive degenerative cycle.

3. METHODS

3.1 Setup design

A custom-made microscope objective was used to split the collected fluorescence arising from angles higher and lower than the critical angle. For a glass-water refractive index discontinuity, this critical angle (θ_c) is 61°, according to the formula $\theta_c = \arcsin(n_{water}/n_{glass})$[62]. Therefore, the objective is designed with an internal parabolic shaped lens able to collect radiation coming from above θ_c for aqueous sample or solution with the same refractive index than water (n = ~1.33). Undercritical angle light is transmitted through a collection of lenses whose numerical aperture is equal to 1.0, which is also used to focus the excitation light. The custom-made objective is mounted on an inverted Olympus IX71. The excitation light source is a power tunable diode laser emitting at 633 nm (TOPTICA iBeam Smart). Optical parts are assembled to drive the collected SAF/UAF fluorescence light simultaneously as two concentric collimated beams. They are separated afterwards toward their respective detector. The constant splitting between two detectors allows the comparison between the signals mentioned before. See the paper by Verders et al. for a detailed description of the optical setup[28].

3.2. Lipids and peptides handling

1,2-dioleoyl-*sn*-glycero-3-phosphocholine (DOPC) and 1,2-Dioleoyl-*sn*-glycero-3-phospho-L-serine (DOPS) in chloroform were used as received (Avanti Polar Lipids). Fluorescently labelled 1,2-dioleoyl-*sn*-glycero-3-phosphoethanolamine powder (DOPE-Atto647; Atto-tec) was diluted in chloroform. A mixture of 65% DOPC / 35% DOPS was used in the SLB, whose protocol had been optimized and already applied to other SLB-peptide studies[29,63]. When experiments required fluorescent SLB, DOPE-Atto647 was added to the lipids mixture to achieve a mass ratio of 1/62500. This amount was determined to give an optimum fluorescence signal with the SAF technique. The following protocol was used for both fluorescent and non-fluorescent SLB. The lipid solution was stirred under nitrogen then left under vacuum (10 mbar) overnight to remove any trace of solvent. Dried lipids were resuspended in degassed "membrane buffer" (NaCl (100 mM), $CaCl_2 \cdot 3H_2O$ (5 mM), Tris (10 mM), pH 7.4; Sigma Aldrich) and extruded at least 20 times through a porous membrane (0.1 µm pore size) to yield unilamellar vesicles with a homogeneous size distribution. The vesicles solution was then diluted in the membrane buffer to a concentration of 0.1 mg/mL and passed through a circulating flow system (0.25 mL/min) connected to the sample plate. A glass coverslip was glued on this sample plate after cleaning (cycle of Deconex11, ethanol and Milli-Q water in ultrasonic bath) and O_2 plasma treatment in order to make the coverslip surface more hydrophilic. When the lipid vesicles adsorbed on this coverslip reached a critical concentration, vesicles

fused to form a SLB. Non-disrupted vesicles were removed by extensive washing with the membrane buffer. Finally, SLB was let to stabilize for at least one hour with PBS (Sigma Aldrich) before any measurement.

Monomeric Aβ (1-40), Aβ (1-42), Aβ (1-40)-Hylite™ Fluor 647 and Aβ (1-42)-Hylite™ Fluor 647 (Anaspec) were reconstituted in a 1% NH_4OH solution, then immediately diluted in PBS. Non-labelled peptides were aliquoted at a concentration of 1 mg/mL and kept at -20°C until use (before 6 months of aging). Labelled peptides were aliquoted at the desired concentration and kept frozen until use.

3.3 Fluorescence measurements

Images of fluorescently labelled SLB or peptide were recorded using the custom-made microscope described previously. Both SAF and UAF signals are collected simultaneously. SAF channel only detects photons arising from the interface vicinity (~200 nm) while UAF channel detects photons emitted from the bulk solution (up to ~2.5 µm) by the use of confocal optics. The sample is constituted of a metal cell plate, whose volume is approximately 200 µL and samples were kept under constant flow rate of 0.25 mL/min with the desired peptide solution during measurements. Fast scanning of the sample area was performed via remote control of a mechanical moving frame.

In order to analyze the mobility of the lipids inside the SLB, fluorescence correlation spectroscopy (FCS) was performed in combination with the supercritical angle collection. Briefly, the method consists to measure fluorescence signal fluctuations due to fluorophores motion within a defined detection volume and to correlate its value over an increasing time lap[30,64]. The radius of the SAF detection volume was calculated to be 550 ± 50 nm by measuring the intensity profile of fluorescent nanoparticles[65]. The persistence of the signal after an increasing delay was fitted with a 2-dimensional diffusion model[66]. Fitting allowed calculation of a diffusion coefficient (D_L) which quantifies the lateral diffusion of lipid molecules (Equations 3, 4). The following equations introduce two diffusion coefficients (D_a and D_b), either to account for two leaflets moving differently or for errors that occur at higher τ values. These errors arise when the measuring time is too short to compensate all irregularities. However, short measuring time can be necessary when targeting a specific fluorescent aggregate moving along the SLB.

$$G(\tau) = a \cdot G_0 \cdot \frac{1}{1+4D_a/\omega_0^2 \cdot \tau} + (1-a) \cdot G_0 \cdot \frac{1}{1+4D_b/\omega_0^2 \cdot \tau} . \quad (3)$$

$$D_L = a \cdot D_a + (1-a)\, D_b . \quad (4)$$

Where G is the autocorrelation value, G_0 is the value at the y intercept, τ is the time delay for the autocorrelation and ω_0 being the radius of the detection volume. The signal was monitored during 1 minute for every FCS measurement. FCS curves were fitted with a Matlab program coded specifically.

Abbreviations

Aβ : Amyloid-Beta, FCS : fluorescence correlation spectroscopy, PBS : phosphate buffer saline, SAF : supercritical angle fluorescence, SLB : supported lipid bilayer, UAF : undercritical angle fluorescence.

Authors information

Valentin Dubois :
valentin.dubois@chem.uzh.ch
Department of Chemistry, University of Zürich, Winterthurerstrasse 190, CH-8057 Zürich, Switzerland

Diana Serrano :
diana.serrano@chimieparistech.psl.eu

Stefan Seeger :

sseeger@chem.uzh.ch
Department of Chemistry, University of Zürich, Wintherthurerstrasse 190, CH-8057 Zürich, Switzerland

Acknowledgment

This work was supported by the Swiss National Science Foundation and the University of Zurich.

Supporting informations

S1. SAF imaging of the adsorption of Aβ on SLB during the short-time adsorption or initial incubation time.

S2. SAF imaging of the adsorption of Aβ on bare glass slide or SLB.

S3. SAF imaging of the adsorption of Aβ on bare glass slide or SLB (2).

S4. SAF and UAF imaging of two types of fluorescent SLB after incubation with Aβ.

S5. FCS curves of fluorescent SLB incubated with 50 μM Aβ(1-40).

S6. FCS curves of fluorescent Aβ aggregates (10 μM) incubated on SLB.

REFERENCES

1. Dinner, A. R.; Šali, A.; Smith, L. J.; Dobson, C. M.; Karplus, M. (2000) Understanding protein folding via free-energy surfaces from theory and experiment. Trends in Biochemical Sciences, 25, 331–339, DOI: 10.1016/S0968-0004(00)01610-8.

2. Dobson, C. M. (2003) Protein folding and misfolding. Nature, 426, 884–890, DOI: 10.1038/nature02261.

3. Clark, P. L. (2004) Protein folding in the cell: Reshaping the folding funnel. Trends in Biochemical Sciences, 29, 527–534, DOI: 10.1016/j.tibs.2004.08.008.

4. Thomas, P. J.; Qu, B.-H.; Pedersen, P. L. (1995) Defective protein folding as a basis of human disease. Trends in Biochemical Sciences, 20, 456–459, DOI: 10.1016/S0968-0004(00)89100-8.

5. Sunde, M.; Serpell, L. C.; Bartlam, M.; Fraser, P. E.; Pepys, M. B.; Blake, C. C. (1997) Common core structure of amyloid fibrils by synchrotron X-ray diffraction. Journal of molecular biology, 273, 729–739, DOI: 10.1006/jmbi.1997.1348.

6. Jahn, T. R.; Makin, O. S.; Morris, K. L.; Marshall, K. E.; Tian, P.; Sikorski, P.; Serpell, L. C. (2010) The common architecture of cross-beta amyloid. Journal of molecular biology, 395, 717–727, DOI: 10.1016/j.jmb.2009.09.039.

7. A. S. Cohen, E. Calkins. (1959) Electron microscopic observation on a fibrous component in amyloid of diverse origins. Nature, 183, 1202–1203.

8. Peter T. Lansbury, JR. (1999) Evolution of amyloid: What normal protein folding may tell us about fibrillogenesis and disease. Proc. Natl. Acad. Sci. USA, 96, 3342–3344.

9. Masters, C. L.; Simms, G.; Weinman, N. A.; Multhaup, G.; McDonald, B. L.; Beyreuther, K. (1985) Amyloid plaque core protein in Alzheimer disease and Down syndrome. Proceedings of the National Academy of Sciences, 82, 4245–4249, DOI: 10.1073/pnas.82.12.4245.

10. O'Brien, R. J.; Wong, P. C. (2011) Amyloid precursor protein processing and Alzheimer's disease. Annual review of neuroscience, 34, 185–204, DOI: 10.1146/annurev-neuro-061010-113613.

11. Muresan, V.; Ladescu Muresan, Z. (2015) Amyloid-beta precursor protein: Multiple fragments, numerous transport routes and mechanisms. Experimental cell research, 334, 45–53, DOI: 10.1016/j.yexcr.2014.12.014.

12. Lee, J. P.; Stimson, E. R.; Ghilardi, J. R.; Mantyh, P. W.; Lu, Y.-A.; Felix, A. M.; Llanos, W.; Behbin, A.; Cummings, M. (1995) 1H NMR of A.beta. Amyloid Peptide Congeners in Water Solution. Conformational Changes Correlate with Plaque Competence. Biochemistry, 34, 5191–5200, DOI: 10.1021/bi00015a033.

13. Tomaselli, S.; Esposito, V.; Vangone, P.; van Nuland, N. A. J.; Bonvin, A. M. J. J.; Guerrini, R.; Tancredi, T.; Temussi, P. A.; Picone, D. (2006) The alpha-to-beta conformational transition of Alzheimer's Abeta-(1-42) peptide in aqueous media is reversible: A step by step conformational analysis suggests the location of beta conformation seeding. Chembiochem : a European journal of chemical biology, 7, 257–267, DOI: 10.1002/cbic.200500223.

14. Giacomelli, C. E.; Norde, W. (2005) Conformational changes of the amyloid beta-peptide (1-40) adsorbed on solid surfaces. Macromolecular bioscience, 5, 401–407, DOI: 10.1002/mabi.200400189.

15. Caughey, B.; Lansbury, P. T. (2003) Protofibrils, pores, fibrils, and neurodegeneration: Separating the responsible protein aggregates from the innocent bystanders. Annual review of neuroscience, 26, 267–298, DOI: 10.1146/annurev.neuro.26.010302.081142.

16. Lambert, M. P.; Barlow, A. K.; Chromy, B. A.; Edwards, C.; Freed, R.; Liosatos, M.; Morgan, T. E.; Rozovsky, I.; Trommer, B.; Viola, K. L. et al. (1998) Diffusible, nonfibrillar ligands derived from A 1-42 are potent central nervous system neurotoxins. Proceedings of the National Academy of Sciences, 95, 6448–6453, DOI: 10.1073/pnas.95.11.6448.

17. Näslund, J. (2000) Correlation Between Elevated Levels of Amyloid β-Peptide in the Brain and Cognitive Decline. JAMA, 283, 1571, DOI: 10.1001/jama.283.12.1571.

18. Smith, D. G.; Cappai, R.; Barnham, K. J. (2007) The redox chemistry of the Alzheimer's disease amyloid beta peptide. Biochimica et biophysica acta, 1768, 1976–1990, DOI: 10.1016/j.bbamem.2007.02.002.

19. Ian V. J. Murray, Michael E. Sindoni, and Paul H. Axelsen. (2005) Promotion of Oxidative Lipid Membrane Damage by Amyloid β Proteins. Biochemistry, 44, 12606–12613.

20. Sasahara, K.; Morigaki, K.; Shinya, K. (2013) Effects of membrane interaction and aggregation of amyloid β-peptide on lipid mobility and membrane domain structure. Physical chemistry chemical physics : PCCP, 15, 8929–8939, DOI: 10.1039/c3cp44517h.

21. M. Kawahara,N. Arispe, Y. Kuroda, and E. Rojas. (1997) Alzheimer's Disease Amyloid (8-Protein Forms Zn2+ Sensitive, Cation-Selective Channels Across Excised Membrane Patches from Hypothalamic Neurons. Biophysical journal, 73, 67–75.

22. Sciacca, Michele F M; Kotler, S. A.; Brender, J. R.; Chen, J.; Lee, D.-k.; Ramamoorthy, A. (2012) Two-step mechanism of membrane disruption by Aβ through membrane fragmentation and pore formation. Biophysical journal, 103, 702–710, DOI: 10.1016/j.bpj.2012.06.045.

23. Khan, M. S.; Dosoky, N. S.; Williams, J. D. (2013) Engineering lipid bilayer membranes for protein studies. International journal of molecular sciences, 14, 21561–21597, DOI: 10.3390/ijms141121561.

24. Czogalla, A.; Grzybek, M.; Jones, W.; Coskun, U. (2014) Validity and applicability of membrane model systems for studying interactions of peripheral membrane proteins with lipids. Biochimica et biophysica acta, 1841, 1049–1059, DOI: 10.1016/j.bbalip.2013.12.012.

25. Richter, R. P.; Berat, R.; Brisson, A. R. (2006) Formation of solid-supported lipid bilayers: An integrated view. Langmuir : the ACS journal of surfaces and colloids, 22, 3497–3505, DOI: 10.1021/la052687c.

26. J. Enderlein, T. Ruckstuhl, and S. Seeger. (1999) Highly efficient optical detection of surface-generated fluorescence. Appl. Opt., 38, 724–732.

27. T. Ruckstuhl, D. Verdes. (2004) Supercritical angle fluorescence (SAF) microscopy. Optic express, 12, 4246–4254.

28. D. Verdes, T. Ruckstuhl, S. Seeger. (2007) Parallel two-channel near- and far-field fluorescence microscopy. J. Biomed. Opt. 12(3).

29. Reynolds, N. P.; Soragni, A.; Rabe, M.; Verdes, D.; Liverani, E.; Handschin, S.; Riek, R.; Seeger, S. (2011) Mechanism of membrane interaction and disruption by α-synuclein. Journal of the American Chemical Society, 133, 19366–19375, DOI: 10.1021/ja2029848.

30. Ries, J.; Ruckstuhl, T.; Verdes, D.; Schwille, P. (2008) Supercritical angle fluorescence correlation spectroscopy. Biophysical journal, 94, 221–229, DOI: 10.1529/biophysj.107.115998.

31. Joseph T. Jarrett, Elizabeth P. Berger, and Peter T. Lansbury, Jr. (1993) The Carboxy Terminus of the Amyloid Protein Is Critical for the Seeding of Amyloid Formation: Implications for the Pathogenesis of Alzheimer's Disease. Biochemistry, 32, 4693–4697.

32. Esbjörner, E. K.; Chan, F.; Rees, E.; Erdelyi, M.; Luheshi, L. M.; Bertoncini, C. W.; Kaminski, C. F.; Dobson, C. M.; Kaminski Schierle, G. S. (2014) Direct observations of amyloid β self-assembly in live cells provide insights into differences in the kinetics of Aβ(1-40) and Aβ(1-42) aggregation. Chemistry & biology, 21, 732–742, DOI: 10.1016/j.chembiol.2014.03.014.

33. Quinn, S. D.; Dalgarno, P. A.; Cameron, R. T.; Hedley, G. J.; Hacker, C.; Lucocq, J. M.; Baillie, G. S.; Samuel, I. D. W.; Penedo, J. C. (2014) Real-time probing of β-amyloid self-assembly and inhibition using fluorescence self-quenching between neighbouring dyes. Molecular bioSystems, 10, 34–44, DOI: 10.1039/c3mb70272c.

34. Rabe, M.; Verdes, D.; Zimmermann, J.; Seeger, S. (2008) Surface organization and cooperativity during nonspecific protein adsorption events. The journal of physical chemistry. B, 112, 13971–13980, DOI: 10.1021/jp804532v.

35. Rabe, M.; Verdes, D.; Seeger, S. (2011) Understanding protein adsorption phenomena at solid surfaces. Advances in colloid and interface science, 162, 87–106, DOI: 10.1016/j.cis.2010.12.007.

36. Daly, S. M.; Przybycien, T. M.; Tilton, R. D. (2003) Coverage-Dependent Orientation of Lysozyme Adsorbed on Silica. Langmuir, 19, 3848–3857, DOI: 10.1021/la026690x.

37. Wertz, C. F.; Santore, M. M. (2002) Adsorption and Reorientation Kinetics of Lysozyme on Hydrophobic Surfaces. Langmuir, 18, 1190–1199, DOI: 10.1021/la0108813.

38. B. Soreghan, J. Kosmoski, C. Glabe. (1994) Surfactant Properties of Alzheimer's ABeta-Peptides and the Mechanism of Amyloid Aggregation. The Journal of biological chemistry, 269.

39. Liu, Y.; Shen, L. (2008) From Langmuir kinetics to first- and second-order rate equations for adsorption. Langmuir : the ACS journal of surfaces and colloids, 24, 11625–11630, DOI: 10.1021/la801839b.

40. Matsuzaki, K. (2007) Physicochemical interactions of amyloid beta-peptide with lipid bilayers. Biochimica et biophysica acta, 1768, 1935–1942, DOI: 10.1016/j.bbamem.2007.02.009.

41. Ariga, T.; Kobayashi, K.; Hasegawa, A.; Kiso, M.; Ishida, H.; Miyatake, T. (2001) Characterization of high-affinity binding between gangliosides and amyloid beta-protein. Archives of biochemistry and biophysics, 388, 225–230, DOI: 10.1006/abbi.2001.2304.

42. D. L. Miller, I. A. Papayannopoulos, J. Styles. (1993) Peptide Composition of the Cerebrovascular and Senile Plaque Core Amyloid Deposits of Alzheimer disease. Archives of biochemistry and biophysics, 301.

43. T. Iwatsubo, A. Odaka, N. Suzuki. (1994) Visualization of AB42(43) and AB40 in Senile Plaques with End-Specific AB Monoclonals: Evidence that an Initially Deposited Species Is AB42(43). Neuron, 13, 45–53.

44. A. Quist, I. Doudevski, H. Lin, R. Azimova. (2005) Amyloid ion channels: A common structural link for protein-misfolding disease. PNAS, 102, 10427–10432.

45. Karran, E.; Mercken, M.; Strooper, B. de. (2011) The amyloid cascade hypothesis for Alzheimer's disease: an appraisal for the development of therapeutics. Nature reviews. Drug discovery, 10, 698–712, DOI: 10.1038/nrd3505.

46. Daniel Axelrod. (1983) Lateral Motion of Membrane Proteins and Biological Function. Membrane Biology, 75, 1–10.

47. Nicolson, G. L. (2014) The Fluid-Mosaic Model of Membrane Structure: still relevant to understanding the structure, function and dynamics of biological membranes after more than 40 years. Biochimica et biophysica acta, 1838, 1451–1466, DOI: 10.1016/j.bbamem.2013.10.019.

48. Przybylo, M.; Sýkora, J.; Humpolíckova, J.; Benda, A.; Zan, A.; Hof, M. (2006) Lipid diffusion in giant unilamellar vesicles is more than 2 times faster than in supported phospholipid bilayers under identical conditions. Langmuir : the ACS journal of surfaces and colloids, 22, 9096–9099, DOI: 10.1021/la061934p.

49. Scomparin, C.; Lecuyer, S.; Ferreira, M.; Charitat, T.; Tinland, B. (2009) Diffusion in supported lipid bilayers: influence of substrate and preparation technique on the internal dynamics. The European physical journal. E, Soft matter, 28, 211–220, DOI: 10.1140/epje/i2008-10407-3.

50. Ding, H.; Schauerte, J. A.; Steel, D. G.; Gafni, A. (2012) β-Amyloid (1-40) peptide interactions with supported phospholipid membranes: a single-molecule study. Biophysical journal, 103, 1500–1509, DOI: 10.1016/j.bpj.2012.08.051.

51. Khachaturian, Z. S. (1987) Hypothesis on the Regulation of Cytosol Calcium Concentration and the Aging Brain. Neurobiology of Aging, 8, 345–346, DOI: 10.1016/0197-4580(87)90073-X.

52. M. P. Mattson, B. Cheng, D. Davis, K. Bryant, I. Lieberburg, and R. E. Rydel. (1992) B-Amyloid Peptides Destabilize Calcium Homeostasis and Render Human Cortical Neurons Vulnerable to Excitotoxicity. the journal of neuroscience, 376–389.

53. Arispe, N., Pollard, H. B. & Rojas. (1993) Giant multilevel cation channels formed by Alzheimer disease amyloid beta-protein [A beta (1-40)] in bilayer membranes. Proc. Nati. Acad. Sci. USA, 90, 567–571.

54. Kagan, B. L.; Azimov, R.; Azimova, R. (2004) Amyloid peptide channels. The Journal of membrane biology, 202, 1–10, DOI: 10.1007/s00232-004-0709-4.

55. H. W. Querfurth, D. J. Selkoe. (1994) Calcium Ionophore Increases Amyloid .beta. Peptide Production by Cultured Cells. Biochemistry, 33, 4550–4561.

56. Itkin, A.; Dupres, V.; Dufrêne, Y. F.; Bechinger, B.; Ruysschaert, J.-M.; Raussens, V. (2011) Calcium ions promote formation of amyloid β-peptide (1-40) oligomers causally implicated in neuronal toxicity of Alzheimer's disease. PloS one, 6, e18250, DOI: 10.1371/journal.pone.0018250.

57. Yu, X.; Zheng, J. (2012) Cholesterol promotes the interaction of Alzheimer β-amyloid monomer with lipid bilayer. Journal of molecular biology, 421, 561–571, DOI: 10.1016/j.jmb.2011.11.006.

58. Hortschansky, P.; Schroeckh, V.; Christopeit, T.; Zandomeneghi, G.; Fändrich, M. (2005) The aggregation kinetics of Alzheimer's beta-amyloid peptide is controlled by stochastic nucleation. Protein science : a publication of the Protein Society, 14, 1753–1759, DOI: 10.1110/ps.041266605.

59. Lockhart, C.; Klimov, D. K. (2015) Calcium enhances binding of Aβ monomer to DMPC lipid bilayer. Biophysical journal, 108, 1807–1818, DOI: 10.1016/j.bpj.2015.03.001.

60. Lau, T.-L.; Ambroggio, E. E.; Tew, D. J.; Cappai, R.; Masters, C. L.; Fidelio, G. D.; Barnham, K. J.; Separovic, F. (2006) Amyloid-beta peptide disruption of lipid membranes and the effect of metal ions. Journal of molecular biology, 356, 759–770, DOI: 10.1016/j.jmb.2005.11.091.

61. Terzi, E.; Hölzemann, G.; Seelig, J. (1997) Interaction of Alzheimer beta-amyloid peptide(1-40) with lipid membranes. Biochemistry, 36, 14845–14852, DOI: 10.1021/bi971843e.

62. Winterflood, C. M.; Ruckstuhl, T.; Verdes, D.; Seeger, S. (2010) Nanometer axial resolution by three-dimensional supercritical angle fluorescence microscopy. Physical review letters, 105, 108103, DOI: 10.1103/PhysRevLett.105.108103.

63. Rabe, M.; Soragni, A.; Reynolds, N. P.; Verdes, D.; Liverani, E.; Riek, R.; Seeger, S. (2013) On-surface aggregation of α-synuclein at nanomolar concentrations results in two distinct growth mechanisms. ACS chemical neuroscience, 4, 408–417, DOI: 10.1021/cn3001312.

64. Elson, E. L.; Magde, D. (1974) Fluorescence correlation spectroscopy. I. Conceptual basis and theory. Biopolymers, 13, 1–27, DOI: 10.1002/bip.1974.360130102.

65. C. M. Winterflood. PhD. Thesis. University of Zürich.

66. Heinemann, F.; Betaneli, V.; Thomas, F. A.; Schwille, P. (2012) Quantifying lipid diffusion by fluorescence correlation spectroscopy: a critical treatise. Langmuir : the ACS journal of surfaces and colloids, 28, 13395–13404, DOI: 10.1021/la302596h.